8-28-2004

Analyses of the Spring Dust Storm Frequency of Northern China in Relation to Antecedent and Concurrent Wind, Precipitation, Vegetation, and Soil Moisture Conditions

Xiaodong Liu

Zhi-Yong Yin

Xiaoye Zhang

Xuchao Yang

Analyses of the spring dust storm frequency of northern China in relation to antecedent and concurrent wind, precipitation, vegetation, and soil moisture conditions

Xiaodong Liu

State Key Laboratory of Loess and Quaternary Geology, Institute of Earth Environment, Chinese Academy of Sciences, Xi'an, China

Zhi-Yong Yin

Marine Science and Environmental Studies, University of San Diego, San Diego, California, USA

Xiaoye Zhang and Xuchao Yang

State Key Laboratory of Loess and Quaternary Geology, Institute of Earth Environment, Chinese Academy of Sciences, Xi'an, China

Received 6 February 2004; revised 6 May 2004; accepted 14 May 2004; published 28 August 2004.

[1] The relationships between the spring (March–May) dust storm frequency (DSF) of northern China, gridded precipitation based on gauge observations, wind velocity at different geopotential heights, satellite-measured land vegetation index, and grid box soil moisture data during 1982–2001 are examined using correlation analysis and singular value decomposition methods. The results show that the spring DSF time series has strong positive correlations with the upwind wind velocity but strong negative correlations with the antecedent summer (June–August) and annual (June of the prior year to May of the current year) precipitation and soil moisture anomalies, as well as with the spring vegetation condition across a region running northeast-southwest from the northeast China and China-Mongolia border to the Taklimakan Desert. This region has been identified as the major source of dust emission in northern China. The results suggest that the summer rainfall anomaly over an extensive area close to the China-Mongolia border is the primary factor that determines the local soil moisture condition in the summer and then the vegetation condition in the following spring through persistence of the soil moisture, eventually determining the variation pattern of the spring DSF in northern China. *INDEX TERMS:* 0305 Atmospheric Composition and Structure: Aerosols and particles (0345, 4801); 1866 Hydrology: Soil moisture; 3309 Meteorology and Atmospheric Dynamics: Climatology (1620); 3354 Meteorology and Atmospheric Dynamics: Precipitation (1854); *KEYWORDS:* dust storm frequency, wind velocity, precipitation, NDVI, soil moisture, China

Citation: Liu, X., Z.-Y. Yin, X. Zhang, and X. Yang (2004), Analyses of the spring dust storm frequency of northern China in relation to antecedent and concurrent wind, precipitation, vegetation, and soil moisture conditions, *J. Geophys. Res.*, *109*, D16210, doi:10.1029/2004JD004615.

1. Introduction

[2] Dust storms, as a natural phenomenon occurring frequently in arid and semiarid regions, are recognized as having a wide range of climatic and environmental impacts. The atmospheric dust loading may play an important role in climate forcing by altering the radiation balance [*Miller and Tegen*, 1998] or affecting cloud microphysics [*Levin et al.*, 1996]. Mineral dust is also believed to have impacts on the nutrient dynamics and marine biogeochemical cycling processes [*Falkowski et al.*, 1998; *Bishop et al.*, 2002]. Moreover, since dust can be transported thousands of kilometers from its sources, the effect of dust storms can be felt in regions far away from their origins [*Goudie and Middleton*, 2001]. As an indictor of overall environmental changes, dust storm frequencies have been used to measure the progress of desertification, vegetation change, and the impact of human activities in arid and semiarid regions [*Zhang et al.*, 2003; *Goudie and Middleton*, 2001; *Qian and Zhu*, 2001].

[3] The region along the border between northern China and Mongolia, with an arid climate and large areas of sandy and gobi (gravel) deserts and sandy lands (Figure 1), is one of the world's largest sources of atmospheric dust [*Prospero et al.*, 2002; *Washington et al.*, 2003]. Studies have shown that spring (March–May) is the season with most frequent dust storms in China, making up to more than 80% of the annual dust storm frequency (DSF) (Figure 1). Every spring, large quantities of dust are generated in northern China by

0148-0227/04/2004JD004615

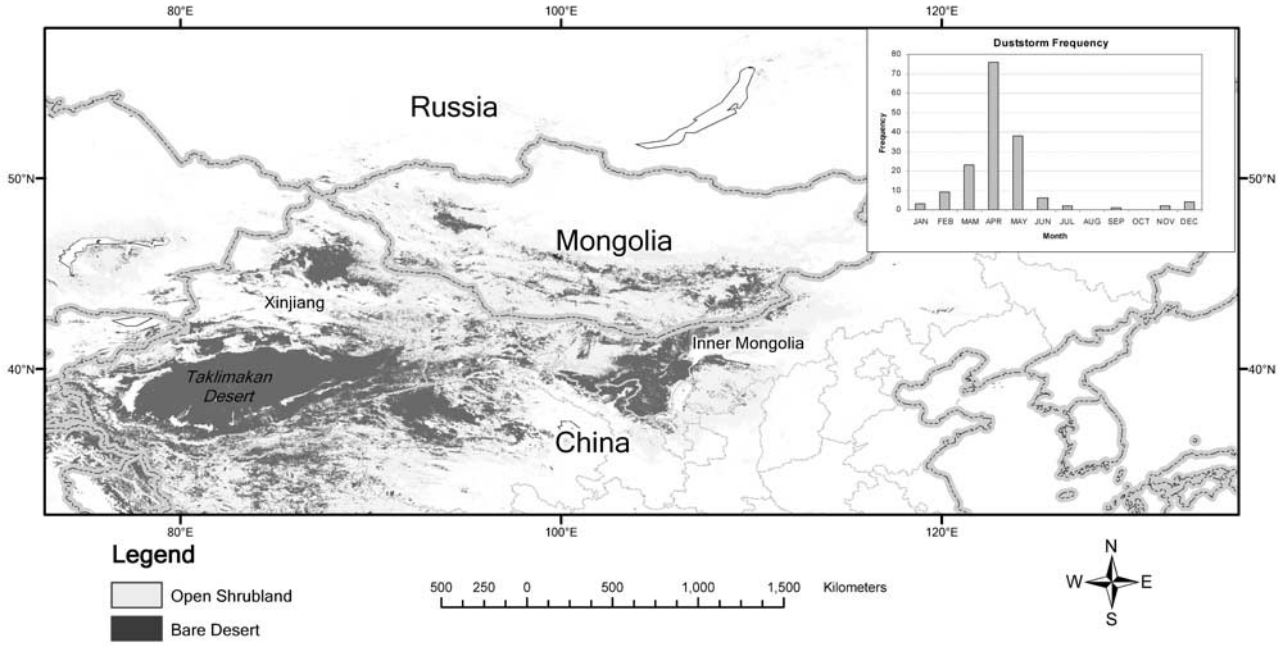

Figure 1. Study region. The distribution of desert landscape is based on the 1-km global land cover classification using advanced very high resolution radiometer data from 1992 to 1993 [*Hansen et al.*, 2000]. The data set was obtained from the Department of Geography, Global Land Cover Facility, University of Maryland, College Park, (http://glcf.umiacs.umd.edu/data/landcover/index.shtml). The classes of barren deserts and open shrub land are presented, which correspond well to the distribution of sandy and gobi deserts in the region. The 20-year-averaged monthly total numbers of weather stations of northern China hit by severe dust storm events are shown in the upper right corner.

cyclonic activities and cold surges that emerge from Siberia [*Goudie and Middleton*, 1992; *Littmann*, 1991; *Qian et al.*, 2002]. According to an estimate by *Xuan et al.* [2000] the total annual dust emission of northern China is approximately 25 million tons, and the spring dust emission accounts for more than half of the annual amount. Also, it has been estimated that that about 800 Tg of dust is injected into the atmosphere annually over China, which may be as much as half of the global production of dust [*Zhang et al.*, 1997]. The dust particles lifted from northern China into the atmosphere can cause local and regional air quality hazards with significant effect on human health [*Kwon et al.*, 2002; *Taylor*, 2002], although the exact effect is still under investigation [*Schwartz et al.*, 1999; *Mage*, 2000]. Furthermore, dust particles can be transported over long distances to as far as Europe, the North Pacific, and even North America [*Grousset et al.*, 2003; *Bishop et al.*, 2002; *McKendry et al.*, 2001]. In addition, studies of dust storms may provide insight into the palaeoenvironmental changes, such as the formation of the Chinese loess deposits [*Derbyshire et al.*, 1998].

[4] Climate is generally regarded as an important factor influencing the occurrence of dust storms. *Goudie* [1983] calculated correlation coefficients between annual DSF and precipitation for different parts of the world. *Littmann* [1991] examined the relationship of the Asian DSF with precipitation, temperature, wind speed, and other climatic parameters and found generally negative correlations to rainfall and positive correlations to wind. *McTainsh et al.* [1998] explored the climatic controls on dust storm occurrence in eastern Australia. They disputed the claim that precipitation is the controlling factor of dust storm occurrence. Instead, they proposed soil moisture as the real controlling factor. *Huang and Gao* [2001] employed an index based on annual wind movement, precipitation, and evaporation and illustrated the influence of climate and a proxy of soil moisture on dust storm occurrence in Maowusu Desert of Inner Mongolia, northern China.

[5] Because of their significance in influencing regional environment, economic activity, and human health, dust storms of China have attracted an increasing attention in recent years, especially the events during springs after 2000, during which often the entire east Asia was affected [*Huebert et al.*, 2003; *Mikami et al.*, 2002]. *Sun et al.* [2001] investigated spatial and temporal characteristics of dust storms in China and its surrounding regions during 1960–1999. The Gobi Desert and Taklimakan Desert were identified as two major source regions. *Yoshino* [2002] studied climatology of dust storms in east Asia including China, Korea, and Japan and ascribed the decrease in the spring DSF of northern China partially to the recent global warming. Another study on dust storm occurrence in Mongolia showed that the number of dusty days has tripled from the 1960s to 1980s and then decreased since 1990 [*Natsagdorj et al.*, 2003]. *Qian et al.* [2002] analyzed the spatial-temporal changes of dust storms in China from 1954 to 1998 and the relevant atmospheric circulation characteristics. They found that the dust weather frequency is closely related to cyclonic activity and cold surge events but only weakly correlated with annual precipitation. They also suggested that the decreasing trend of DSF in China during the past few decades could be attributed to the decreased

cyclone frequency in northern China due to the reduced meridional temperature gradient. *Shao and Wang* [2003] examined the spring dust storm activities of northeast Asia including China using 2000–2002 surface meteorological records. The regions with frequent dust events were found in the Tarim Basin, southern Mongolia, and Inner Mongolia, and Hexi Corridor of China.

[6] To date, the most reliable and comprehensive climatological analysis of Chinese dust storms has been performed by *Zhou and Zhang* [2003]. Their results indicate that severe dust storms mainly occurred in the Tarim Basin, the eastern part of northwest China, and the northern part of north China. Although the DSF of northern China has a general decreasing tendency during the past decades [*Zhou and Zhang*, 2003], the recent few years (2000–2003) have seen an alarming increase in the DSF in east Asia [*Kurosaki and Mikami*, 2003; *Gao et al.*, 2003]. The main cause was considered to be the strengthening of surface winds [*Kurosaki and Mikami*, 2003] or the decrease in annual precipitation [*Gao et al.*, 2003].

[7] In general, previous studies have demonstrated intricate relations between climate and DSF. However, the climate control of the DSF has not been fully understood, especially the physical linkage between climatic variables, such as precipitation, and DSF. In this paper, we will examine the relationship of the spring DSF of northern China to macroscale precipitation and wind patterns, vegetation condition, and soil moisture in the midlatitude Asian continent to clarify the time and region in which precipitation exerts the strongest influence on the DSF. We also want to explore the physical processes that link precipitation patterns and the DSF. We hope that the results of this study will be helpful to the medium- to long-range prediction of dust storms in China.

2. Data and Method

[8] Five different data sets were used in this study.

2.1. Time Series of Spring Severe Dust Storm Frequency in Northern China

[9] *Zhou and Zhang* [2003] constructed a time series of typical severe dust storms in northern China by using original daily meteorological records of dust storms and relevant data of high wind and visibility from 681 weather stations over a period of 49 years (1954–2002). For each station, daily wind and visibility data were used to rank the days of dust storm events as severe, moderate, and weak. Then a regional criterion was used to identify the typical severe dust storm in northern China: During the same weather process, (1) three or more stations registered severe dust storm events; or (2) two stations registered severe dust storms, and three or more stations registered moderate dust storm events; or (3) only one station registered a severe dust storm event, but five or more stations registered moderate dust storm events.

[10] On the basis of the data set presented by *Zhou and Zhang* [2003], we obtained a spring DSF time series in northern China by calculating the total number of weather stations where typical severe dust storm events were observed for each spring (March, April, and May). The data for the 20 springs during 1982–2001 were then selected to match the other data sets available for analysis.

2.2. Wind Velocity at Different Geopotential Heights

[11] We extracted the wind velocity data as the composite of the meridional and zonal flow components from the National Centers for Environment Prediction–Department of Energy (NCEP-DOE) data set, NCEP-DOE Reanalysis 2 [*Kanamitsum et al.*, 2002]. This is an updated version of the NCEP/National Center for Atmospheric Research (NCAR) data set, NCEP/NCAR Reanalysis, a widely used data set containing multiple atmospheric variables at different geopotential heights, including wind, temperature, pressure (geopotential heights), and humidity. We considered data from five different height levels: 500 (middle troposphere), 600, 700, and 850 hPa and surface (10 m).

2.3. Gridded Precipitation Based on Gauge Observations

[12] The 1981–2001 monthly land precipitation data on a $1^\circ \times 1^\circ$ grid [*Chen et al.*, 2002] were used as the basic data set of precipitation for this paper. This gridded field of monthly precipitation is produced by interpolating gauge observations at over 15,000 stations in the world using the optimum interpolation algorithm [*Chen et al.*, 2002]. On the basis of this data set we calculated the seasonal and annual mean precipitation rates (mm/d) for each grid of the midlatitude Asian continent region as shown in Figure 1. Note that the annual mean values used in this study are the averages from June of the prior year to May of the current year, which is different from the means of calendar years. For example, the annual mean value of 1982 is the average from June 1981 to May 1982.

2.4. Satellite-Based Land Vegetation Index

[13] The normalized difference vegetation index (NDVI) derived from the advanced very high resolution radiometer on the National Oceanic and Atmospheric Administration (NOAA) polar-orbiting satellite has been widely used as an indicator of the vegetation activity. NDVI is calculated using the reflectance in the red (R) and near infrared (NIR) spectral bands [*Lillesand and Kiefer*, 2000]:

$$\mathrm{NDVI} = (\mathrm{NIR} - \mathrm{R})/(\mathrm{NIR} + \mathrm{R}).$$

For surfaces covered with rigorous vegetation, the NDVI tends to have values close to +1.0. For surfaces with poor vegetation cover or no vegetation cover the NDVI tends to be negative or close to −1.0. In the present study, the spring mean NDVI data with a $1^\circ \times 1^\circ$ resolution for 1982–2001 were utilized [*James and Kalluri*, 1994].

2.5. Grid Box Soil Moisture Data From the Reanalysis Data

[14] The NCEP-DOE Reanalysis Project (Reanalysis 2) uses an analysis/forecast system (Reanalysis Data Assimilation System) to perform assimilation on data since 1979 [*Kanamitsum et al.*, 2002]. The Reanalysis 2 data have markedly reduced biases than the previous reanalysis data for water balance calculations, especially for soil moisture. We extracted volumetric soil moisture data (fractal) every 6 hours in the top 10 cm of soil and in the 10- to 200-cm

layer and then computed seasonal and annual mean relative soil moisture for the 1.9° × 1.9° grids.

[15] In this study, we first calculated correlation coefficients to examine the simultaneous and lag relationships between the spring DSF, wind velocity, precipitation, NDVI, and soil moisture. Meanwhile, the singular value decomposition (SVD) method was employed to reveal the coupled relationship between the patterns of antecedent annual precipitation anomaly, soil moisture, and the spring NDVI. The SVD is a powerful tool to identify sets of linear relations between two fields by decomposing the covariance matrix of the two fields into singular values and two sets of paired orthogonal vectors, one for the "left" field and one for the "right" field. The SVD method maximizes the covariance between the expansion coefficients of the leading patterns in the left and right fields. The results of SVD include the squared covariance fraction (SCF), as the percentage of the total squared covariance explained by a given SVD mode, and the correlation between the time coefficients that are scores in the form of time series to represent the variation of the SVD mode. Detailed treatments of the SVD method and its applications are given by *Bretherton et al.* [1992] and *Liu and Yanai* [2001].

3. Results

3.1. Concurrent Correlations Between the Spring DSF and Surface to Middle Tropospheric Wind Speeds

[16] The relationship between wind speed and dust storm occurrence is well documented since wind is the driving force for dust and sand deflation and transport. Results of our analysis conform to previous studies, finding strong positive correlations between the spring DSF and surface (10 m) wind speed across Mongolia and northern China (Figure 2e). There are three centers of high correlations: the western portion of the Mongolia-Russia border, the eastern portion of the China-Mongolia border, and northwestern China (Hexi Corridor). More interestingly, however, we also found strong correlations between the spring DSF and upper air wind speed (Figures 2a–2d). In fact, there is a gradual shift of the area with strong positive correlations (>0.5) from western Siberia toward Mongolia as the height decreases. The highest correlations are seen for wind speed at middle troposphere levels (500–700 hPa), with the strongest correlations higher than 0.7. Furthermore, this area is not found immediately over northern China where the severe dust storms occurred but for the upwind area over western Siberia. This suggests that while surface wind speed is the direct mechanism of dust emission, the atmospheric conditions conducive to dust storms are very much related to the regional circulation patterns as demonstrated by the upper airflows. High-velocity winds over western Siberia at the middle troposphere level may provide short-term precursor signals for the occurrence of dust storms in northern China. In fact, the outbreaks of cold surges originating from western Siberia during spring time, in combination with suitable surface condition, are regarded as the main cause of dust storms in northern China and Mongolia [*Goudie and Middleton*, 1992; *Littmann*, 1991; *Qian et al.*, 2002]. The above analysis revealed the concurrent relationship between spring DSF and wind speeds. We also examined the correlations between the spring DSF and wind field data in the previous winter and the preceding summer monsoon season, but we did not find any meaningful relationship. In searching for long-range precursor signals of dust storm occurrence we investigated other factors associated with the DSF in sections 3.2–3.4.

3.2. Correlations Between the Antecedent Precipitation Field and the Subsequent Spring DSF

[17] We first examined space-time distribution of precipitation in the study region since precipitation has been identified as a major factor of DSF in previous studies [e.g., *Goudie*, 1983; *Littmann*, 1991]. Figure 3 shows the 20-year mean seasonal and annual precipitation rates. The eastern part of the study region (north China and Mongolia) mostly belongs to the east Asian monsoon climate, where precipitation in a year mainly concentrates in the summer season (Figure 3a). Spatially, precipitation exceeds 2 mm/d in most parts east of 110°E, while a large region with low precipitation (<0.5 mm/d) exists in a belt from the China-Mongolia border to the Taklimakan Desert. Precipitation in the eastern part of the region dramatically decreases from summer to fall, and the area of low precipitation (<0.5 mm/d) enlarges (Figure 3b), while the driest season is winter (Figure 3c). Precipitation begins to increase from winter to spring (Figure 3d) and the distribution of precipitation in spring displays a quite similar pattern to that in the fall. In the field of annual mean precipitation rate (Figure 3e) the area of low precipitation (<0.5 mm/d) occupies a large portion of northwestern China and southwestern Mongolia, with large areas of sandy and gobi deserts (Figure 1). Therefore this area serves as the major eolian dust source region on the Asian continent [*Xuan et al.*, 2000; *Washington et al.*, 2003].

[18] High interannual variability in precipitation is a typical characteristic of arid and semiarid climates, and it tends to produce extreme conditions, such as severe droughts, which significantly affect the regional soil and vegetation conditions. We calculated the ratio of standard deviation to mean of the seasonal and annual precipitation rates to reflect interannual variability (Figure 4). We found that precipitation rates of summer (Figure 4a) and winter (Figure 4c) generally have relatively high interannual variability as compared to those of the transitional seasons (fall and spring) (Figures 4b and 4d). This is the result of the high standard deviation in summer and low mean values in winter. The annual pattern (Figure 4e) approximately resembles the seasonal patterns, although the values in the former are much lower than those of the latter. A common feature in all these patterns is a belt of high interannual variability running northeast-southwest from the China-Mongolia border to the Taklimakan Desert, which very much coincides with the low-precipitation region (<0.5 mm/d) as shown in Figure 3e and the distribution of deserts in Figure 1.

[19] Results of correlation analysis of the seasonal and annual precipitation rates with the DSF time series (Figure 5) suggest that the spring DSF is negatively correlated to precipitation rates of the antecedent and concurrent seasons in most of the study region, especially to the precipitation rates of the antecedent summer and the concurrent spring. The areas with the strongest negative correlations between the spring DSF and the antecedent summer precipitation are located in areas of western Mongolia to eastern Xinjiang,

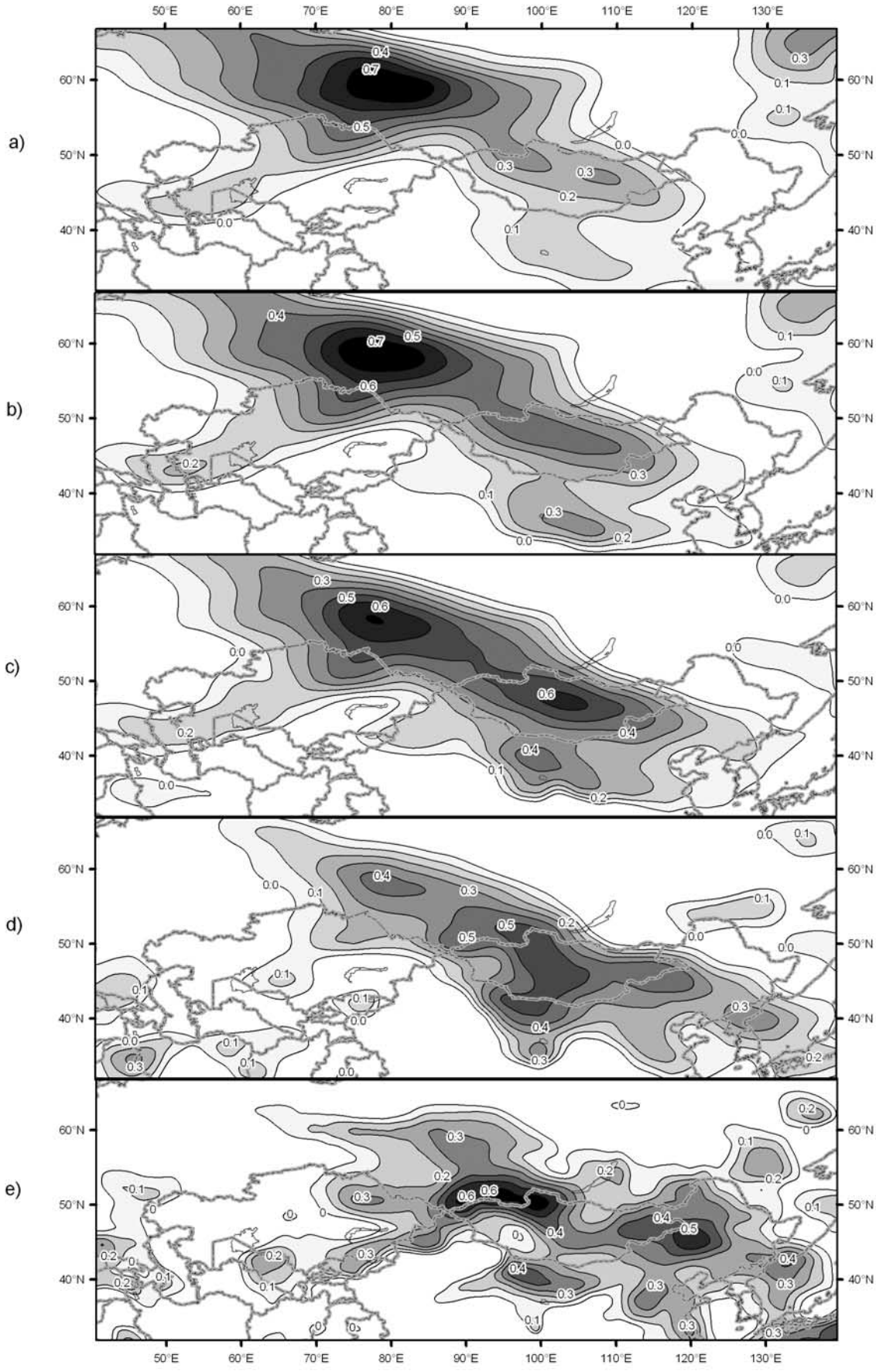

Figure 2

eastern Mongolia to Inner Mongolia, and northeast China. The correlation coefficients at the cores of these areas exceed the value corresponding to the 0.05 significance level (Figure 5a). In the concurrent correlation field between the spring DSF and precipitation rates the strongest negative correlations occur along the middle section of the China-Mongolia border and in southern Xinjiang (Figure 5d), showing a pattern different from the correlation pattern of the antecedent summer precipitation (Figure 5a). Although correlations of the spring DSF with the antecedent fall (Figure 5b) and winter (Figure 5c) are relatively weak and unstable in spatial distribution, the correlation pattern of annual precipitation rates (Figure 5e) is similar to that of the preceding summer precipitation. Moreover, the correlation coefficients between spring DSF and annual precipitation rates are stronger than those of summer precipitation rates in western and eastern Mongolia. This suggests that the summer precipitation anomaly dominates the overall variability of precipitation of the whole year (starting from the summer of the previous year and ending in the end of spring of the current year), but the cumulative effect of the precipitation anomaly of the entire year is by far the most important factor to the spring dust storm occurrence.

[20] For a more intuitive examination of the relationship between the antecedent annual precipitation rates and spring DSF we constructed the composite annual precipitation anomalies (as percentages to the long-term means during 1982–2001) for two springs of the highest DSF (1983 and 2001, as shown in Figure 10) during the study period (Figure 6). It can be seen that the antecedent annual precipitation rates were significantly below normal in a vast area with the China-Mongolia border as its center when dust storms occurred most frequently over northern China. The percentage anomalies of the annual precipitation rates in the central region reached −30% or lower, which were comparable to the levels of precipitation anomalies associated with severe dust storms observed in Inner Mongolia of China [*Gao et al.*, 2003]. It is also interesting to note that the regions with significant below-normal anomalies in the precipitation rates in those two years agree with those of strong correlations between the annual precipitation rates and spring DSF (Figure 5e).

3.3. Relationships of the Spring NDVI With the Concurrent DSF and Antecedent Precipitation

[21] Considering vegetation condition as the most direct control of dust emissions [*Engelstaedter et al.*, 2003], also examined in this study was the relationship of vegetation condition to the dust storm activities. Figure 7a shows the spatial pattern of the 1982–2001 mean spring NDVI. One can observe that the pattern of NDVI generally matches those of the precipitation rates (Figure 3). The high (low) values in the NDVI field, as a whole, correspond to the high (low) values in the precipitation fields. In other words, the vegetation condition is mainly governed by precipitation in the study region.

[22] Figure 7b shows the correlation coefficient between the concurrent spring NDVI and DSF in each grid cell. It is interesting to note the similarity between the patterns of the NDVI-DSF correlation and the precipitation-DSF correlation (Figure 5e). For example, there are significant negative correlations in western and eastern Mongolia, Xinjiang, and the eastern part of northwest China. Furthermore, correlations of the DSF with the NDVI are stronger than those with the precipitation rates overall. This implies that the spring vegetation condition in these key areas may influence the spring dust storm activity in northern China and that it can offer additional explanation as to the occurrence of dust storms over that provided by the antecedent annual cumulative precipitation anomalies alone.

[23] The covariance between the NDVI and precipitation rates at each grid cell may reveal the possible linkages between the antecedent precipitation and the spring vegetation condition, which eventually affect the dust storm occurrence. Figure 8 shows a region with the highest covariance (1982–2001) between the spring NDVI and the corresponding annual precipitation (June of the previous year to May of the current year), running northeast-southwest from the China-Mongolia border to the Taklimakan Desert. This region is consistent with the region of the highest interannual variability of precipitation rates (Figure 4). Such patterns resulted from the nature of vegetation types dominant in the semiarid and arid regions, where vegetation conditions of the steppe grassland and arid shrubs are very sensitive to the antecedent and concurrent moisture conditions.

[24] In order to further explore the linkages between the annual precipitation rates and the spring NDVI the SVD analysis was performed on both fields. The results show that the SCF of the first mode reached 53.1%, with a correlation coefficient of 0.81 between the time coefficients of the two fields (Table 1). The SCF indicates the percentage of the total squared covariance explained by the SVD mode, as a measure of the relative importance of a given SVD mode in the relationship between the two fields [*Bretherton et al.*, 1992]. A SCF of 53.1% implies that this coupled mode reflects more than half of the linear interaction between the annual precipitation rate and the subsequent spring NDVI. The high correlation coefficient of the time coefficients for the first SVD mode indicates that there is a strong relation between the variation in annual precipitation rates and spring vegetation conditions linking dust storm activities. For this reason we focused our further analysis on this most important leading mode of SVD.

[25] The spatial pattern of the first SVD mode for the antecedent annual precipitation and the subsequent spring NDVI anomalies is shown in Figure 9, displaying a generally consistent pattern of variation in a broad region (with high values) extending from northeast China to southern Mongolia and eventually all the way to the Taklimakan Desert in a northeast-southwest direction. This pattern is similar to the pattern of covariance between spring NDVI and annual precipitation rates shown in Figure 8. Thus this

Figure 2. Correlation coefficients between the spring (MAM) dust storm frequency (DSF) in northern China and concurrent wind speeds at various geopotential heights: (a) 500, (b) 600, (c) 700, and (d) 850 hPa and (e) surface (10 m). Only positive correlation coefficients are shown.

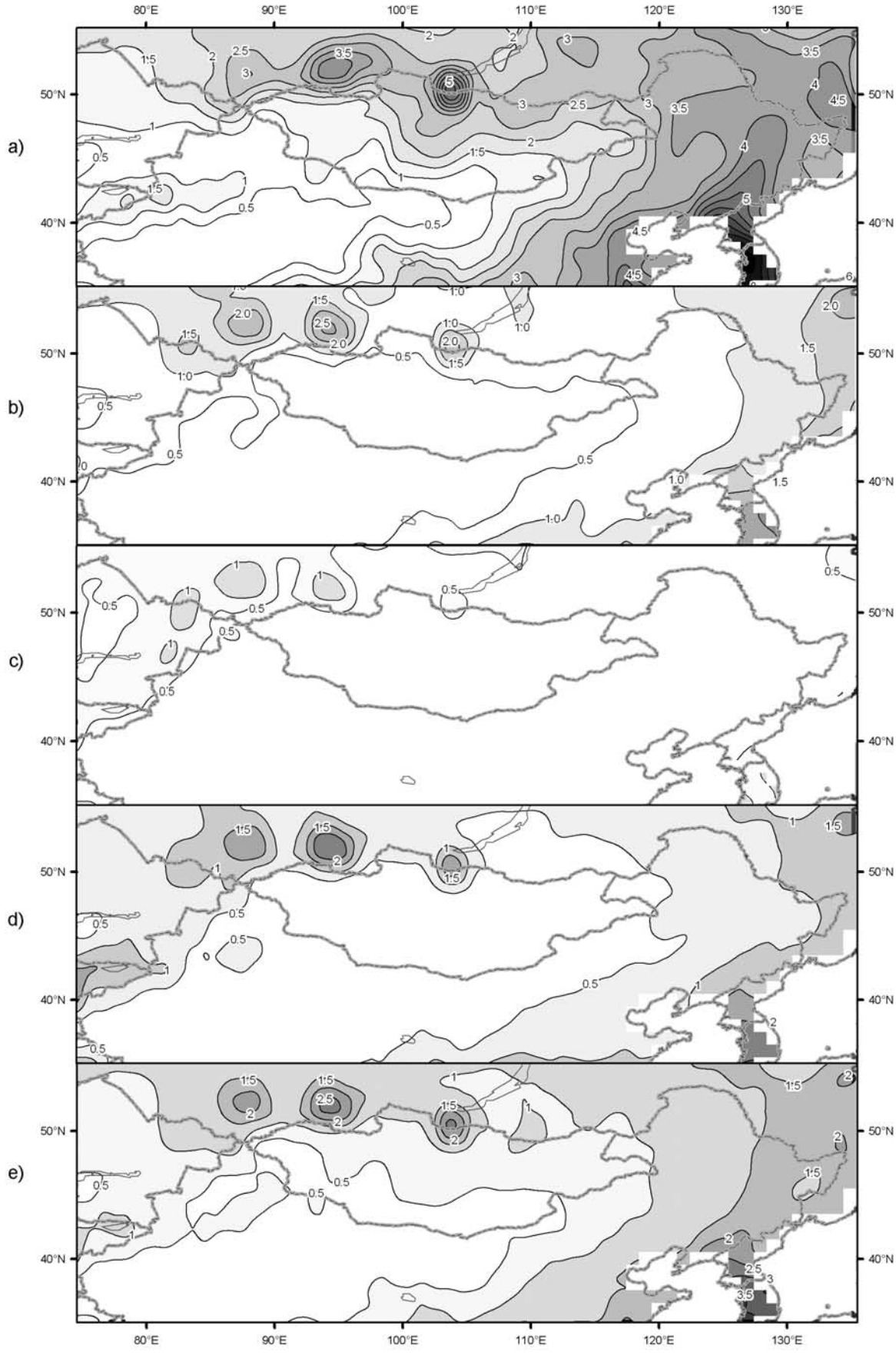

Figure 3

pair of coupled spatial patterns from the SVD analysis again verifies the coherent variation of the spring NDVI (and therefore DSF) with the preceding annual precipitation.

[26] Figure 10 depicts year-to-year time coefficients of the first SVD modes of the spring NDVI and antecedent annual precipitation rate anomalies and the spring DSF anomalies in the study region. The interannual covarying pattern between the SVD modes of spring NDVI and annual precipitation is clear ($r = 0.81$). Additionally, the spring DSF is negatively correlated with the spring NDVI ($r = -0.67$) and the antecedent annual precipitation ($r = -0.57$). The most remarkable feature, however, is the extraordinarily high frequency of dust storms that occurred in the springs of 1983 and 2001, corresponding to the negative time coefficients of the NDVI and the annual precipitation rate anomalies for the first SVD modes. The spatial pattern of the annual precipitation rate anomalies, which were negative in most areas, is shown in Figure 6 of section 3.2.

3.4. Soil Moisture Condition and Its Persistence Associated With the Spring DSF

[27] The linkage between precipitation anomalies and vegetation condition is soil moisture. In arid and semiarid regions the vigor of vegetation is very sensitive to soil moisture conditions. Additionally, increasing soil moisture may promote surface crusting for certain soil types, which may limit dust emission. We first examined the relationships of the spring DSF to antecedent and concurrent seasonal and annual soil moisture conditions in the depth of 0–10 cm. The patterns of the correlation fields between the spring DSF and the soil moisture conditions (Figure 11) are similar to those of the precipitation fields (Figure 5). There are a few centers of strong negative correlations in western and eastern Mongolia and the central part of northern China close to the China-Mongolia border in both seasonal and annual correlation fields. Besides the consistent patterns among these correlation fields it seems that the correlation between the spring DSF and soil moisture displays a more stable pattern in different seasons than that of the precipitation. It is also interesting to note that the correlations between soil moisture and spring DSF are more temporarily consistent in the eastern part of the study region, which is characterized by semiarid to subhumid climates with more dramatic variation in absolute soil moisture.

[28] As illustrated in section 3.2, summer precipitation dominates the annual variation pattern in the study region. Therefore the dominance of summer soil moisture condition should be considered in determining soil moisture persistence. In other words, for areas with strong soil moisture persistence the summer soil moisture condition should have a long-lasting influence in the following months. To evaluate the spatial pattern of soil moisture persistence in the study region, we calculated nine correlation coefficients of the antecedent summer (June–August) soil moisture to the succeeding monthly soil moisture from September to May of next year for every grid cell and then used the mean value of the nine correlation coefficients as a measure of the persistence.

[29] The result shows that the areas of western and eastern Mongolia and the region along the China-Mongolia border display the strongest persistence (Figure 12). We also noticed that these regions of strong persistence approximately overlap the main centers in the correlation fields between the soil moisture and the DSF (Figure 11). In fact, the persistence of antecedent soil moisture anomalies associated with the spring dust storm activity is stronger in a deeper soil layer. Taking soil moisture for the 10- to 200-cm layer averaged for the two main anomalous regions (40°–45°N, 90°–100°E and 40°–45°N, 110°–120°E) for the 1983 and 2001 events as an example, we can see from Figure 13a that all regional mean anomalies of the soil moisture were negative for each month from June 1982 to May 1983 and then from June 2000 to May 2001. In addition, the cumulative anomalies of the monthly soil moisture display linearly downward trends. For the sake of comparison, the monthly anomalies of precipitation averaged for the same regions from June 1982 to May 1983 and then from June 2000 to May 2001 are also presented here (Figure 13b). Strong negative precipitation anomalies only occurred in the antecedent summer, while dust storms broke out with high frequencies in the following spring, forming a striking contrast to the soil moisture condition that clearly offered a more intuitive explanation. This is because soil moisture anomalies, rather than the precipitation anomalies, have a strong persistence from the summer to the following spring, which represents the cumulative impact on vegetation condition during the following months and the emission of dust in spring. Therefore the linkage of the antecedent summer precipitation to the subsequent spring DSF is accomplished by impacting the summer soil moisture condition and eventually through the persistence of the soil moisture anomalies exerting its influence on the following spring DSF. Our results support the viewpoint of *McTainsh et al.* [1998] that "the real control upon dust storms is soil moisture and associated vegetation cover rather rainfall."

4. Conclusions and Discussion

[30] Our results indicate that the spring (March–May) DSF in northern China has strong positive correlations with concurrent surface wind speed, conforming to results of previous studies. We also found that the spring DSF is strongly correlated to the upwind middle tropospheric wind speed over western Siberia, reflecting the link between macroscale circulation patterns and regional atmospheric conditions conducive to dust storm occurrence in northern China. Additionally, we found strong negative correlations of the spring DSF to the antecedent seasonal and annual precipitation rates and soil moisture anomalies, as well as to the spring NDVI variations. Prior to a spring with frequent dust storm events, the preceding summer (June–August)

Figure 3. Climatological distribution of seasonal and annual mean precipitation rates (mm/d): (a) summer (1981–2000 JJA), (b) autumn (1981–2000 SON), (c) winter (1982–2001 DJF), (d) spring (1982–2001 MAM), and (e) annual (June 1981 to May 2001).

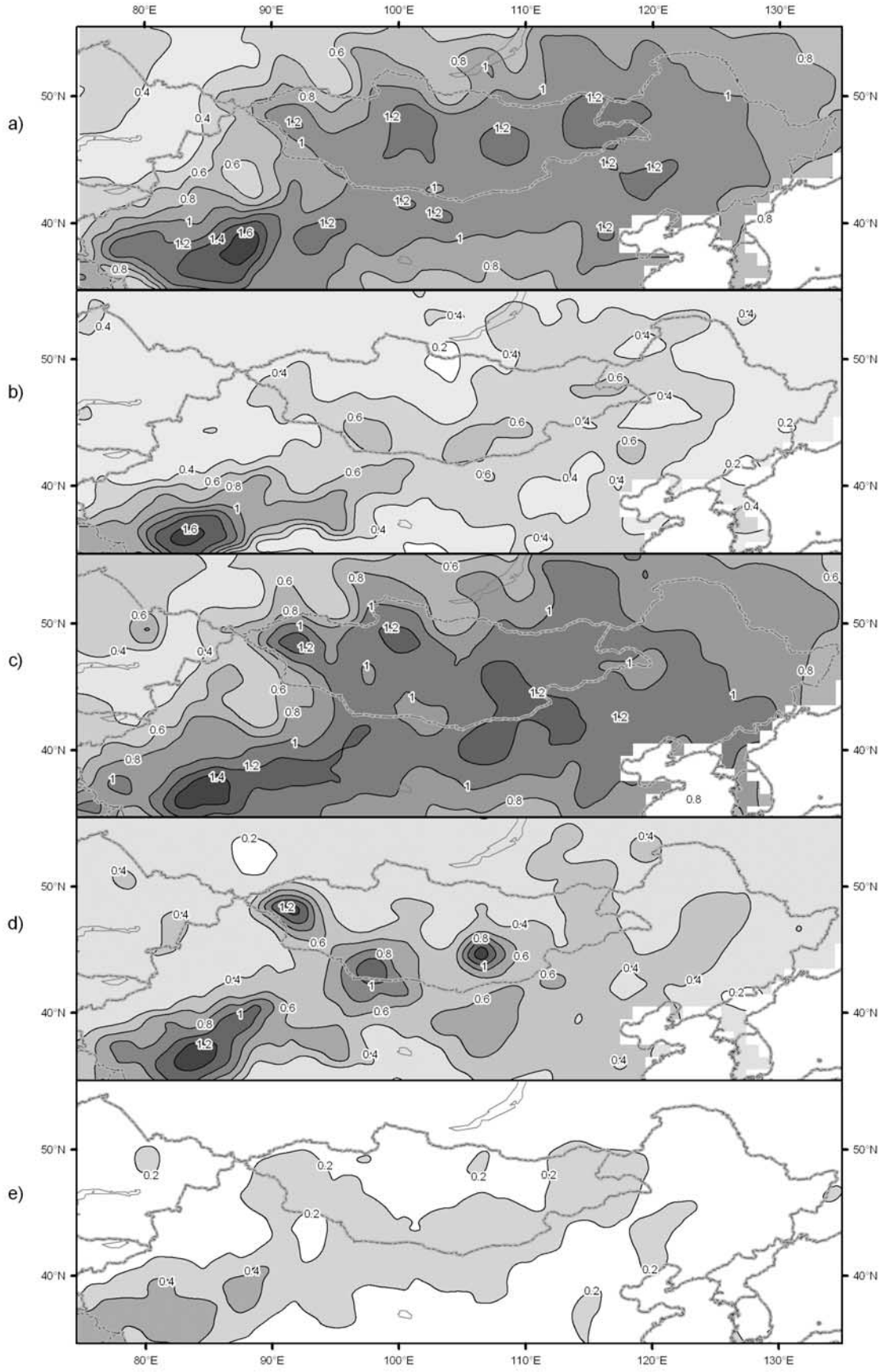

Figure 4. Same as in Figure 3 but for the interannual variability of precipitation as the ratio of the standard deviation to mean.

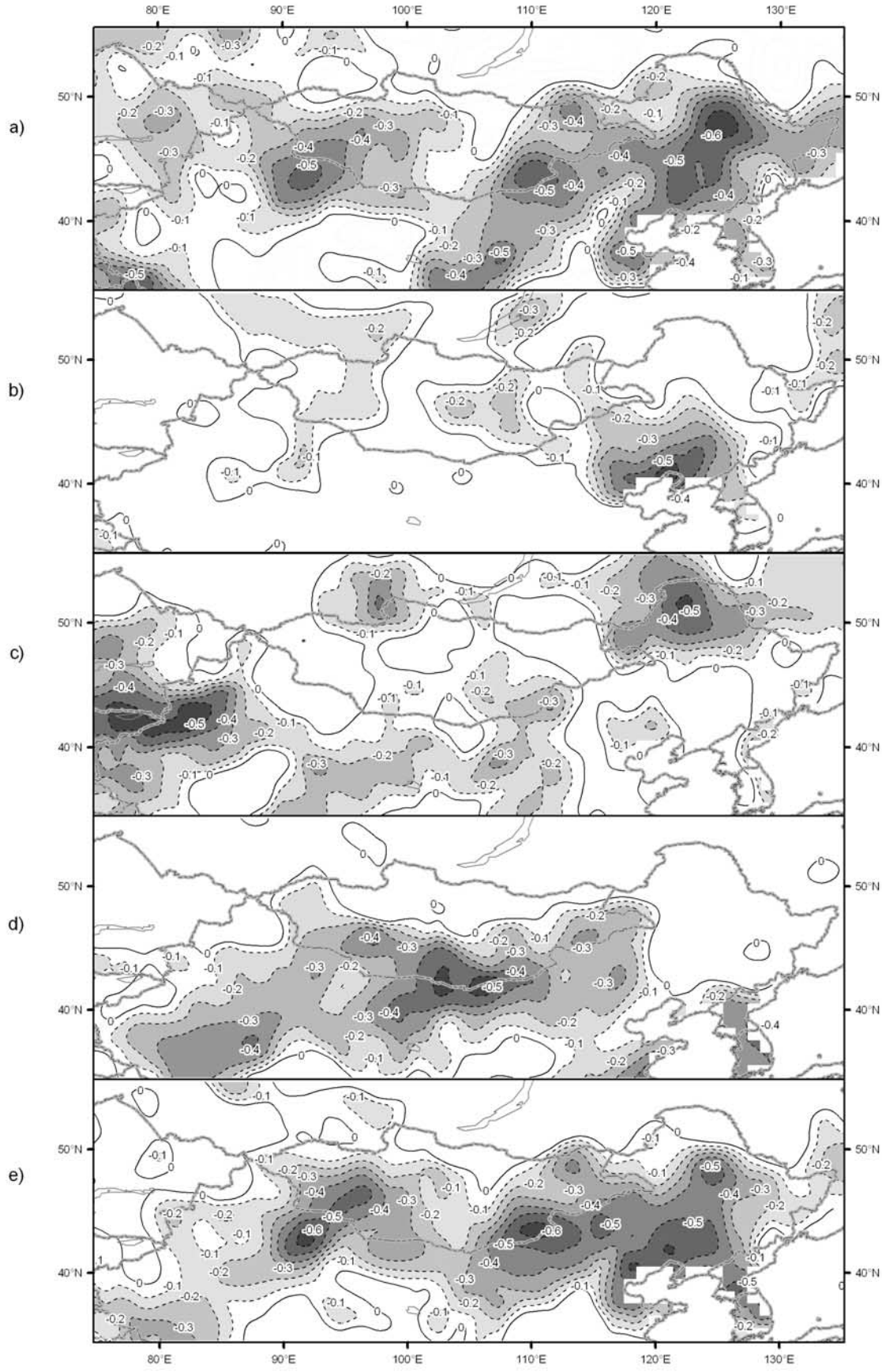

Figure 5. Same as in Figure 3 but for the correlation coefficients of the spring DSF time series with seasonal and annual precipitation at every grid box. Only negative correlation coefficients are shown.

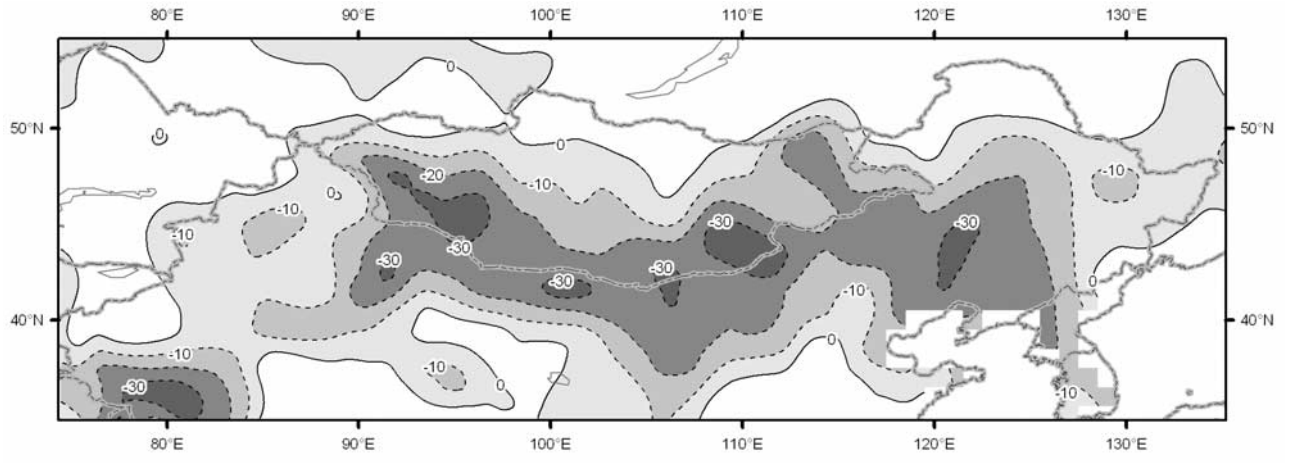

Figure 6. Percentage anomalies of prior annual precipitation (percent), composite in terms of two springs with the highest DSF (1983 and 2001). Only areas with negative anomalies are shown.

and annual (June of the prior year to May of the same year) precipitation is generally below normal in western and eastern Mongolia and most parts of northern China. The antecedent annual precipitation may decrease up to 30% or more below the long-term means in the area along the China-Mongolia border. At the same time the SVD analysis shows that the antecedent precipitation anomaly pattern is coherently coupled with the spring NDVI anomaly pattern, with a correlation coefficient of 0.81 between the two time coefficients of the first SVD mode. More precipitation in the preceding year leads to more flourishing vegetation and low emission of dust in the following spring, especially in a northeast-southwest orientated band from northeast China and the China-Mongolia border to the Taklimakan Desert,

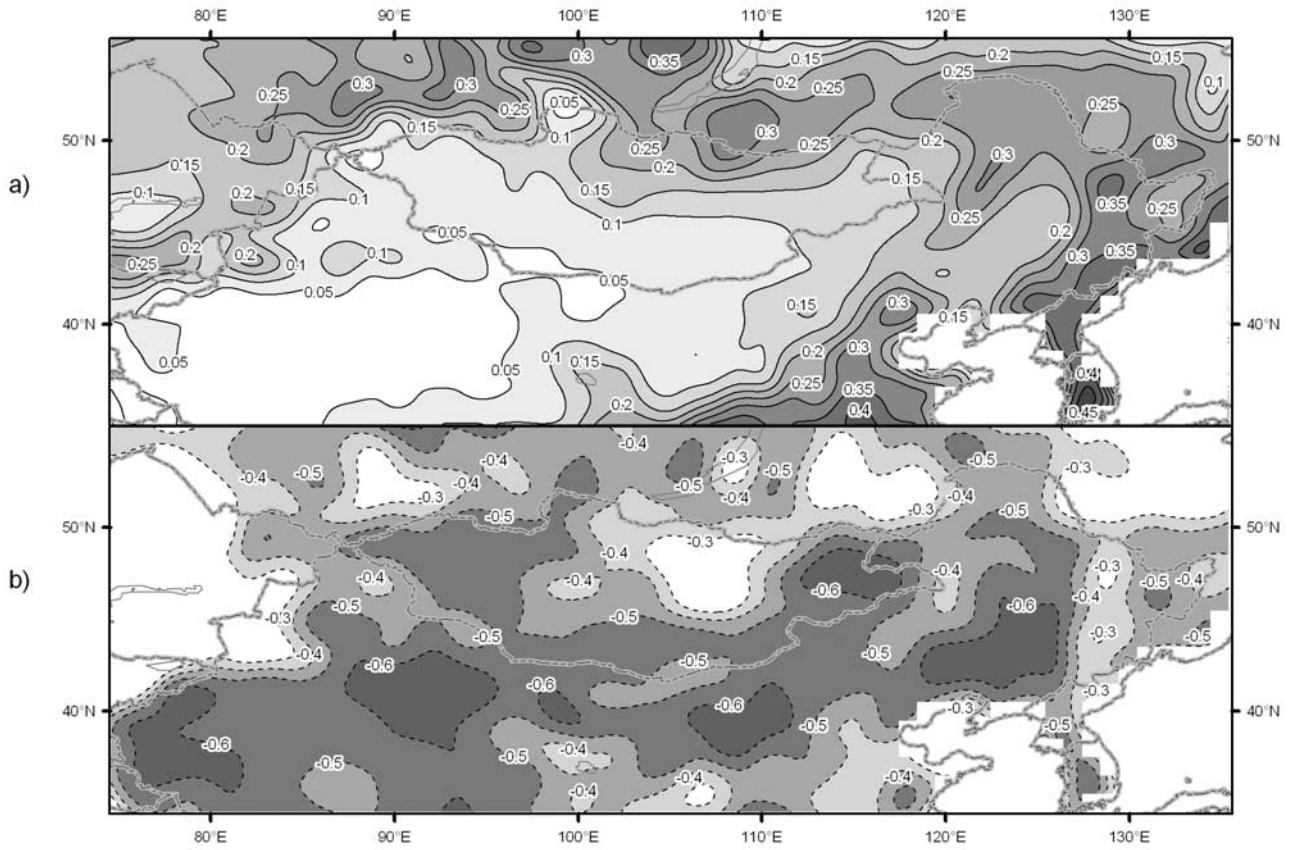

Figure 7. (a) Distribution of the normalized difference vegetation index (NDVI) averaged for the 20 springs during 1982–2001. (b) Correlation coefficients between the gridded spring mean NDVI and the spring DSF time series for 1982–2001. Only correlation coefficients lower than −0.3 are shown.

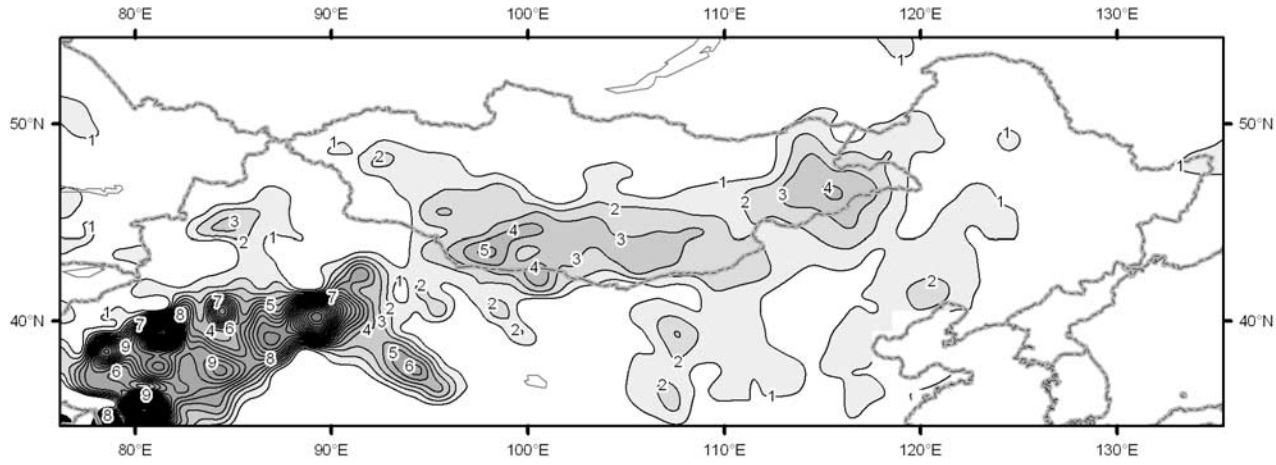

Figure 8. Geographical distribution of covariance (multiplied by 100) between the spring NDVI and the preceding annual (prior June to May of the current year) precipitation for 1982–2001. Only values greater than 1.0 are shown.

approximately corresponding to area with the highest interannual variability of precipitation. The spatial patterns of the correlation between antecedent seasonal or annual soil moisture condition and the spring DSF are found to be similar to those of the precipitation, but the former have a stronger temporal persistence.

[31] Although there are strong negative correlations between the spring DSF and the antecedent precipitation anomalies, which can be used as a precursory signal useful for predicting the dust storm activity in northern China, their cause-effect relationship is not immediately evident. A possible linkage based on our results is that the summer rainfall anomaly in an extensive area close to the China-Mongolia border is primarily responsible for impacting the local soil moisture in that summer, and then the summer soil moisture anomaly influences the vegetation condition in the subsequent spring through its persistence and cumulative effects, eventually determining the variation of the spring DSF of northern China.

[32] These areas of northern China and Mongolia identified in this study, where the antecedent precipitation anomaly is closely related to the subsequent spring dust storm activity, are mostly characterized by sandy and gobi deserts and sandy lands with arid or semiarid climates and vegetation types. They serve as the main source regions of dust storms of northern China [*Prospero et al.*, 2002; *Washington et al.*, 2003]. An arid climate favors the expansion of preferential environments for the production and entrainment of dust. Through various positive feedbacks a random event of a dry summer due to high interannual variability in precipitation may lead to persistent low soil moisture in the following months, reduced vegetation vigor and coverage, and enhanced wind erosion and may produce high dust loads into the atmosphere. Dust entrainment occurs when the wind speed is sufficient to overcome the cohesive forces that exist between soil particles. It is facilitated by low soil moisture levels related to deficient precipitation that reduces the cohesion of soil and affects vegetation cover, which, in turn, allows greater wind speeds at the ground level [*Holcombe et al.*, 1997]. The higher dust fluxes could further reinforce the dryness by suppressing convection [*Rosenfeld et al.*, 2001]. On the other hand, wet years in these source regions could trigger rapid revegetation of desert surfaces, reducing the amount of dust emission into the atmosphere and possibly pushing the climate system toward wetter conditions through similar feedbacks. It is not surprising then to discover that the areas with the strongest correlation between the antecedent precipitation and the spring DSF are predominantly restricted to the arid and semiarid areas with the highest interannual variability of precipitation. Our results suggest that antecedent precipitation and modeled soil moisture conditions can be used as precursor signals in long-range prediction of dust storm occurrence.

[33] Our findings clearly point to soil moisture and its persistence as the linkage between the antecedent precipitation and the subsequent DSF, but further research on the physical processes is needed to establish the validity of the suggested explanations. It should be pointed out that antecedent precipitation is only one of several major factors influencing the spring DSF. To comprehensively understand the spatial and temporal variations of dust storm occurrence, many other influential factors, such as surface winds related to cold surges, vegetation and topography, physical characteristics of soil, and human activities, will have to be taken into account [*Kurosaki and Mikami*, 2003; *Engelstaedter et al.*, 2003; *Zender et al.*, 2003; *Dong et al.*, 2000]. The study region has experienced significant increases in human population in the past decades. With increasing population pressure, intensified animal husbandry and reclamation of

Table 1. Summary of the SVD Analysis for Annual Precipitation Rates and the Spring NDVI[a]

SVD Mode	SCF, %	CC
1	53.14	0.81
2	15.93	0.83
3	6.47	0.82
4	5.00	0.76
5	3.30	0.84

[a]SVD is singular value decomposition; NDVI is normalized difference vegetation index. SCF and CC are squared covariance fraction and correlation coefficient for each SVD mode, respectively.

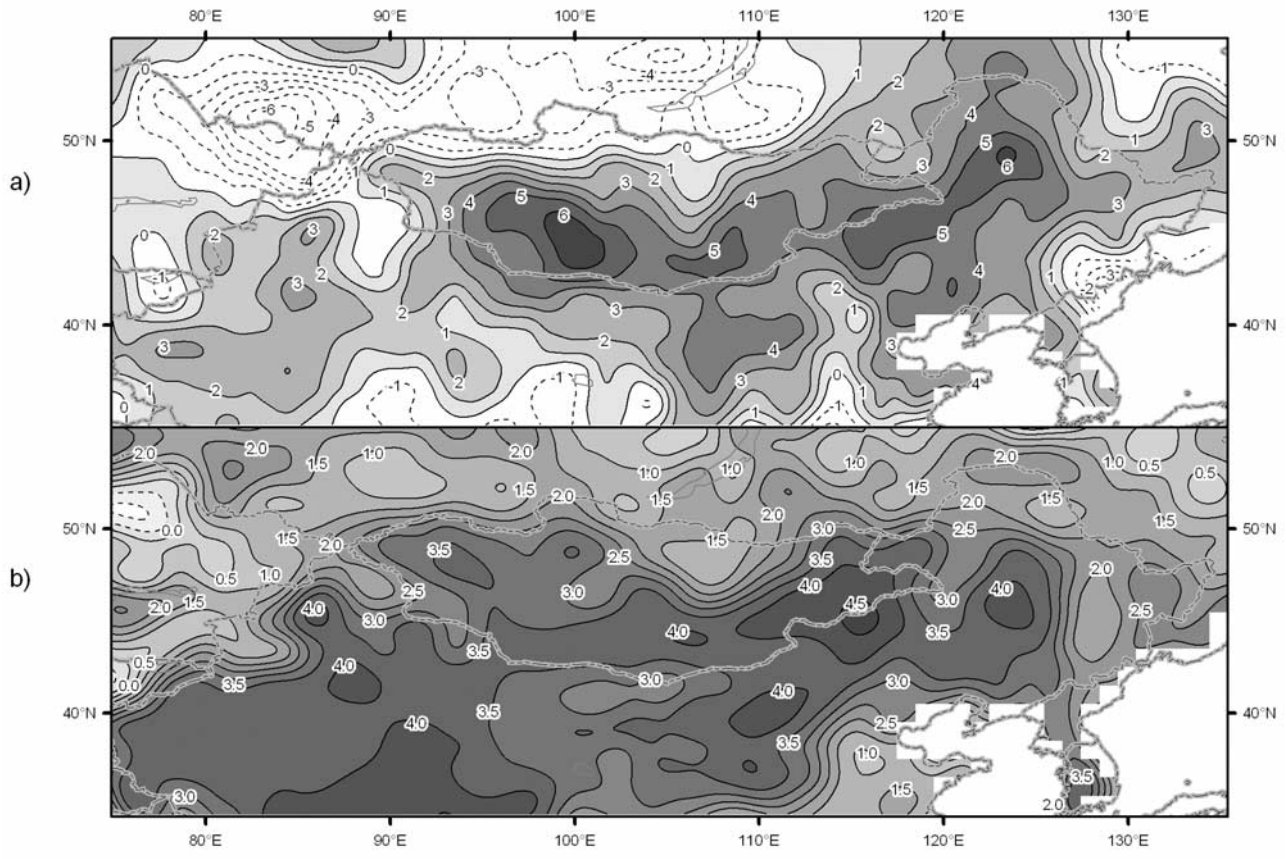

Figure 9. Spatial patterns of the first singular value decomposition (SVD) for the (a) prior annual precipitation and (b) spring NDVI anomalies. The original values are amplified 100 times for the purpose of plotting.

land marginal for farming have been extensively implemented in the study region. For example, in Inner Mongolia alone, the population grew from 6,081,000 in 1949 to 23,448,000 in 1998, while heads of livestock increased from 8,727,900 to 43,902,800 during the same time period [*Wu et al.*, 2002]. There were also several episodes of large-scale land reclamation activities during the 1950s–1970s. Much of the newly reclaimed land was later abandoned, but

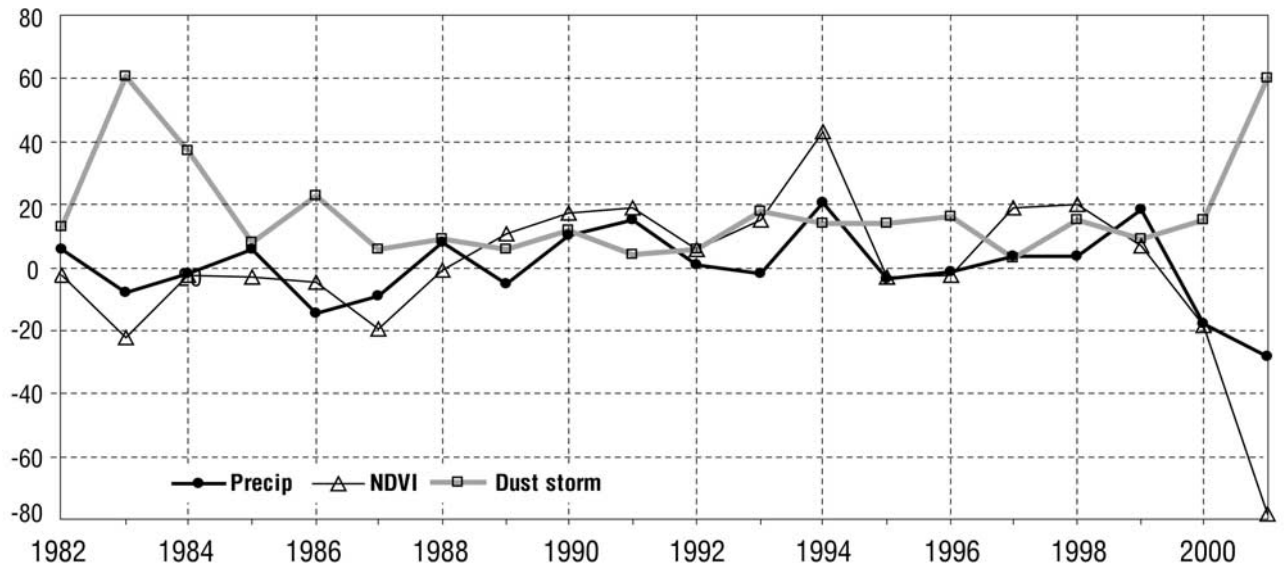

Figure 10. Yearly time coefficients of the first SVD mode for the spring NDVI, those for the preceding annual precipitation anomalies, and the spring DSF series for 1982–2001.

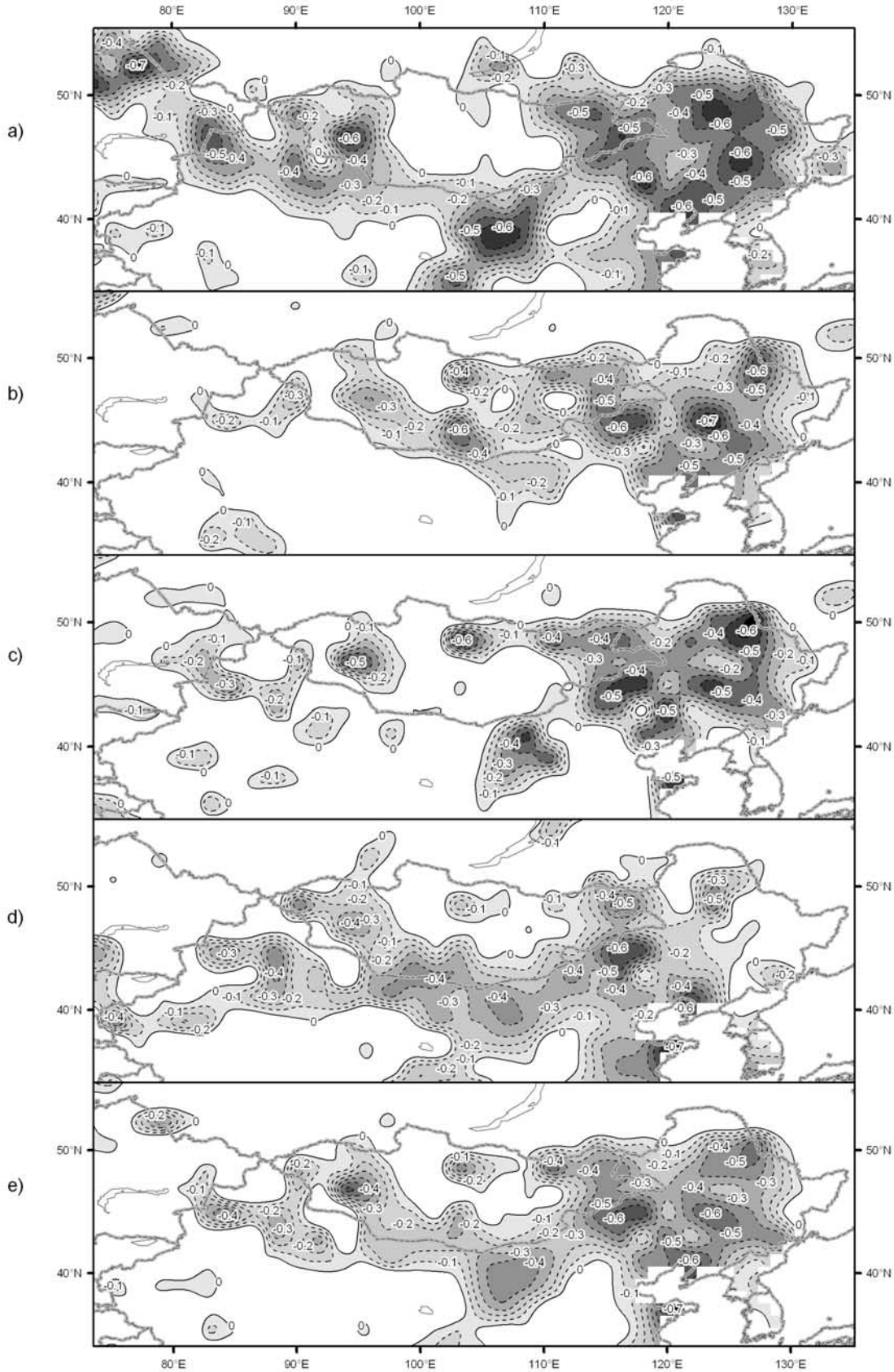

Figure 11. Same as in Figure 3 but for the correlation coefficients of the DSF time series with the seasonal and annual mean soil moisture in the depth of the top 0–10 cm. Only negative correlation coefficients are shown.

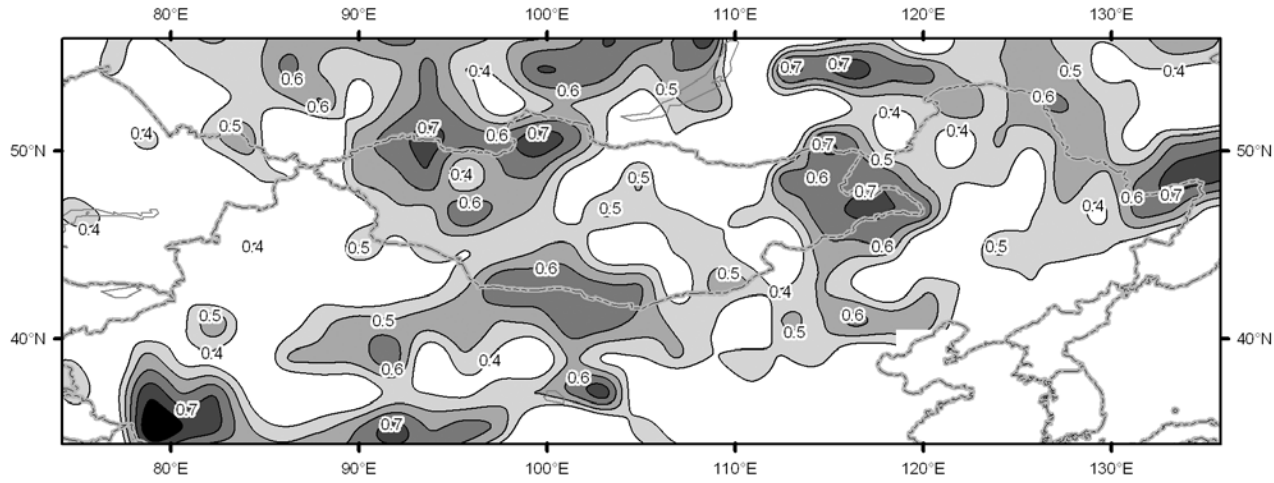

Figure 12. Persistence of the summer 0- to 10-cm soil moisture anomaly (mean correlation coefficients of the summer soil moisture with the succeeding September–May monthly soil moisture). Only regions with strong persistence (correlation coefficients higher than 0.4) are shown.

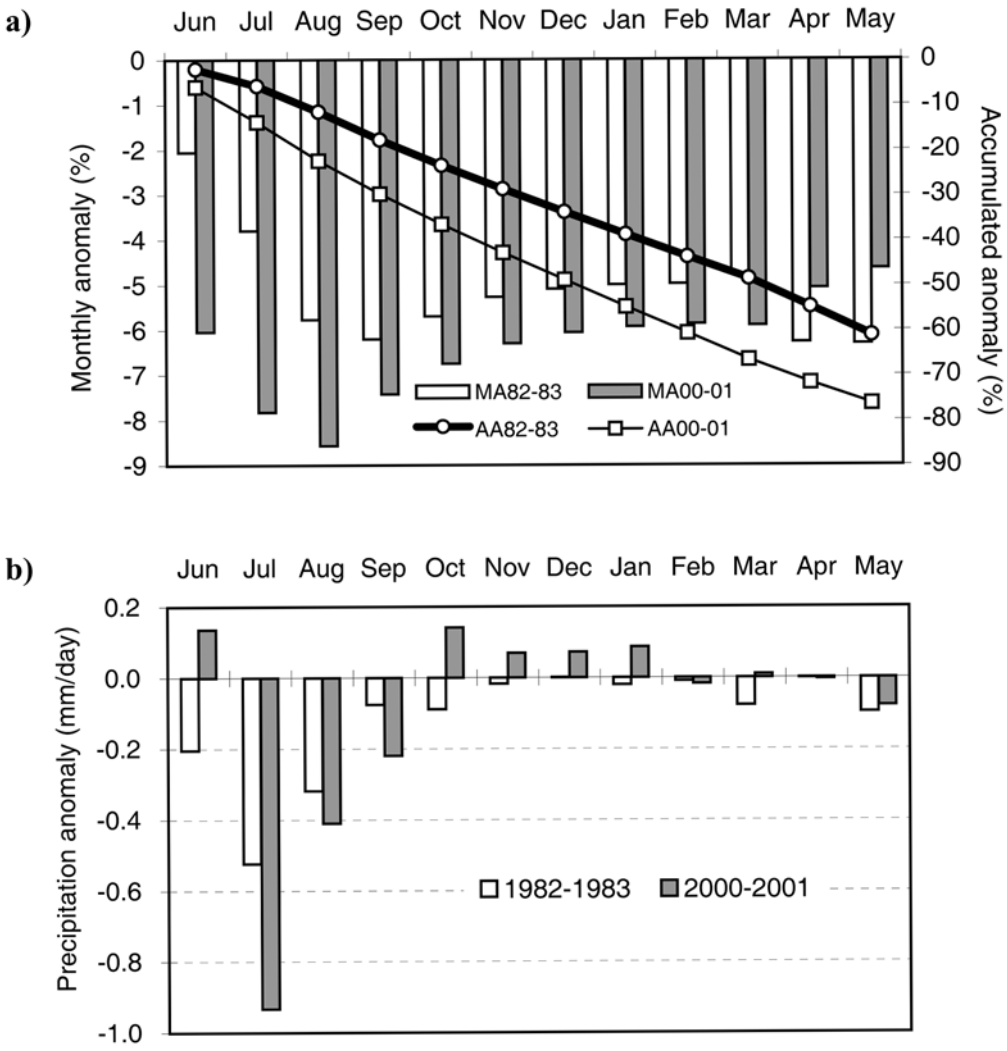

Figure 13. (a) Percentages of monthly anomaly (MA) and accumulated anomaly (AA) of the 10- to 200-cm soil moisture. (b) Monthly anomaly of precipitation from June 1982 to May 1983 and from June 2000 to May 2001, averaged for the two main anomalous regions (40°–45°N, 90°–100°E and 40°–45°N, 110°–120°E).

the continued influence of land reclamation and overgrazing on the regional environment still needs to be investigated. Finally, the relative significance of antecedent precipitation needs to be compared to that of the other factors in controlling the subsequent spring DSF.

[34] **Acknowledgments.** The assistance of G. S. Chen and X. Z. Li in the preparation of this paper is gratefully acknowledged. This study was supported by grants from the Ministry of Science and Technology, Chinese Academy of Sciences, and the Natural Science Foundation of China (G2000048703, KZCX2-SW-118, 2001CCB00100, 2003CCC01500, and NSFC40121303).

References

Bishop, J. K., R. E. Davis, and J. R. Sherman (2002), Robotic observations of dust storm enhancement of carbon biomass in the North Pacific, *Science*, *298*, 817–821.

Bretherton, C. S., C. Smith, and J. M. Wallace (1992), An intercomparison of methods for finding coupled patterns in climate data, *J. Clim.*, *5*, 541–560.

Chen, M., P. Xie, J. E. Janowiak, and P. A. Arkin (2002), Global land precipitation: A 50-yr monthly analysis based on gauge observations, *J. Hydrometeorol.*, *3*, 249–266.

Derbyshire, E., X. M. Meng, and P. A. Kemp (1998), Provenance, transport and characteristics of modern aeolian dust in western Gansu Province, China, and interpretation of the Quaternary loess record, *J. Arid Environ.*, *39*(3), 497–516.

Dong, Z. B., X. M. Wang, and L. Y. Liu (2000), Wind erosion in arid and semiarid China: An overview, *J. Soil Water Conserv.*, *55*(4), 439–444.

Engelstaedter, S., K. E. Kohfeld, I. Tegen, and S. P. Harrison (2003), Controls of dust emissions by vegetation and topographic depressions: An evaluation using dust storm frequency data, *Geophys. Res. Lett.*, *30*(6), 1294, doi:10.1029/2002GL016471.

Falkowski, P. G., R. T. Barber, and V. Smetacek (1998), Biogeochemical controls and feedbacks on ocean primary production, *Science*, *281*, 200–206.

Gao, T., L. J. Su, Q. X. Ma, H. Y. Li, X. C. Li, and X. Yu (2003), Climatic analyses on increasing dust storm frequency in the spring of 2000 and 2001 in Inner Mongolia, *Int. J. Climatol.*, *23*, 1743–1755.

Goudie, A. S. (1983), Dust storms in space and time, *Prog. Phys. Geogr.*, *7*, 502–530.

Goudie, A. S., and N. J. Middleton (1992), The changing frequency of dust storms through time, *Clim. Change*, *20*, 197–225.

Goudie, A. S., and N. J. Middleton (2001), Saharan dust storms: Nature and consequences, *Earth Sci. Rev.*, *56*(1–4), 179–204.

Grousset, F. E., P. Ginoux, A. Bory, and P. E. Biscaye (2003), Case study of a Chinese dust plume reaching the French Alps, *Geophys. Res. Lett.*, *30*(6), 1277, doi:10.1029/2002GL016833.

Hansen, M., R. DeFries, J. R. G. Townshend, and R. Sohlberg (2000), Global land cover classification at 1 km resolution using a decision tree classifier, *Int. J. Remote Sens.*, *21*, 1331–1365.

Holcombe, T. L., T. Ley, and D. A. Gillette (1997), Effects of prior precipitation and source area characteristics on threshold wind velocities for blowing dust episodes, Sonoran Desert 1948–78, *J. Appl. Meteorol.*, *36*, 1160–1175.

Huang, F. X., and Q. Gao (2001), Climate controls on dust storm occurrence in Maowusu Desert, Inner Mongolia, north China, *J. Environ. Sci. China*, *13*, 14–21.

Huebert, B. J., T. Bates, P. B. Russell, G. Shi, Y. J. Kim, K. Kawamura, G. Carmichael, and T. Nakajima (2003), An overview of ACE-Asia: Strategies for quantifying the relationships between Asian aerosols and their climatic impacts, *J. Geophys. Res.*, *108*(D23), 8633, doi:10.1029/2003JD003550.

James, M. E., and S. N. V. Kalluri (1994), The Pathfinder AVHRR land data set: An improved coarse-resolution data set for terrestrial monitoring, *Int. J. Remote Sens.*, *15*, 3347–3363.

Kanamitsum, M., W. Ebisuzaki, J. Woollen, S.-K. Yang, J. J. Hnilo, M. Fiorino, and G. L. Potter (2002), NCEP-DOE AMIP-II Reanalysis (R-2), *Bull. Atmos. Meteorol. Soc.*, *83*(11), 1631–1643.

Kurosaki, Y., and M. Mikami (2003), Recent frequent dust events and their relation to surface wind in east Asia, *Geophys. Res. Lett.*, *30*(14), 1736, doi:10.1029/2003GL017261.

Kwon, H.-J., S.-H. Cho, Y. Chun, F. Lagarde, and G. Pershagen (2002), Effects of the Asian dust events on daily mortality in Seoul, Korea, *Environ. Res.*, *90*, 1–5.

Levin, Z., E. Ganor, and V. Gladstein (1996), The effects of desert particles coated with sulfate on rain formation in the eastern Mediterranean, *J. Appl. Meteorol.*, *35*, 1511–1523.

Lillesand, T. M., and R. W. Kiefer (2000), *Remote Sensing and Image Interpretation*, 4th ed., 724 pp., John Wiley, Hoboken, N. J.

Littmann, T. (1991), Dust storm frequency in Asia: Climatic control and variability, *Int. J. Climatol.*, *11*, 393–412.

Liu, X. D., and M. Yanai (2001), Relationship between the Indian monsoon precipitation and the tropospheric temperature over the Eurasian continent, *Q. J. R. Meteorol. Soc.*, *127*, 909–937.

Mage, D. T. (2000), Coarse particles and dust storm mortality, *Environ. Health Perspect.*, *108*, A12.

McKendry, I. G., J. P. Hacker, R. Stull, S. Sakiyama, D. Mignacca, and K. Reid (2001), Long-range transport of Asian dust to the Lower Fraser Valley, British Columbia, Canada, *J. Geophys. Res.*, *106*(D16), 18,361–18,370.

McTainsh, G. H., A. W. Lynch, and E. K. Tews (1998), Climatic controls upon dust storm occurrence in eastern Australia, *J. Arid Environ.*, *39*(3), 457–466.

Mikami, M., et al. (2002), The impact of aeolian dust on climate: Sino-Japanese cooperative project ADEC, *J. Arid Land Stud.*, *11*(4), 211–222.

Miller, R. L., and I. Tegen (1998), Climate response to soil dust aerosols, *J. Clim.*, *11*(12), 3247–3267.

Natsagdorj, L., D. Jugder, and Y. S. Chung (2003), Analysis of dust storms observed in Mongolia during 1937–1999, *Atmos. Environ.*, *37*, 1401–1411.

Prospero, J. M., P. Ginoux, O. Torres, S. E. Nicholson, and T. E. Gill (2002), Environmental characterization of global sources of atmospheric soil dust identified with the Nimbus 7 Total Ozone Mapping Spectrometer (TOMS) absorbing aerosol product, *Rev. Geophys.*, *40*(1), 1002, doi:10.1029/2000RG000095.

Qian, W., and Y. Zhu (2001), Climate change in China from 1880 to 1998 and its impact on the environmental condition, *Clim. Change*, *50*, 419–444.

Qian, W. H., L. S. Quan, and S. Y. Shi (2002), Variations of the dust storm in China and its climatic control, *J. Clim.*, *15*(10), 1216–1229.

Rosenfeld, D., Y. Rudich, and R. Lahav (2001), Desert dust suppressing precipitation: A possible desertification feedback loop, *Proc. Natl. Acad. Sci. U. S. A.*, *98*(11), 5975–5980.

Schwartz, J., G. Norris, T. Larson, L. Sheppard, C. Claiborne, and J. Koenig (1999), Episodes of high coarse particles concentration are not associated with increased mortality, *Environ. Health Perspect.*, *107*, 339–342.

Shao, Y. P., and J. J. Wang (2003), A climatology of northeast Asian dust events, *Meteorol. Z.*, *12*(4), 187–196.

Sun, J. M., M. Y. Zhang, and T. S. Liu (2001), Spatial and temporal characteristics of dust storms in China and its surrounding regions, 1960–1999: Relations to source area and climate, *J. Geophys. Res.*, *106*(D10), 10,325–10,333.

Taylor, D. A. (2002), Dust in the wind, *Environ. Health Perspect.*, *110*, A80–A87.

Washington, R., M. Todd, N. J. Middleton, and A. S. Goudie (2003), Dust-storm source areas determined by the Total Ozone Monitoring Spectrometer and surface observations, *Ann. Assoc. Am. Geogr.*, *93*(2), 297–313.

Wu, Y. N., H. Pei, and M. L. Bai (2002), Relationship between sandy desertification and climatic change, human activity in the Inner Mongolia (in Chinese), *J. Desert Res.*, *22*(3), 292–297.

Xuan, J., G. L. Liu, and K. Du (2000), Dust emission inventory in northern China, *Atmos. Environ.*, *34*, 4565–4570.

Yoshino, M. (2002), Climatology of yellow sand (Asian sand, Asian dust or Kosa) in east Asia, *Sci. China, Ser. D*, *45*, suppl., 59–70.

Zender, C. S., D. Newman, and O. Torres (2003), Spatial heterogeneity in aeolian erodibility: Uniform, topographic, geomorphic, and hydrologic hypotheses, *J. Geophys. Res.*, *108*(D17), 4543, doi:10.1029/2002JD003039.

Zhang, X. Y., R. Arimoto, and Z. S. An (1997), Dust emission from Chinese desert sources linked to variations in atmospheric circulation, *J. Geophys. Res.*, *102*(D23), 28,041–28,047.

Zhang, X. Y., S. L. Gong, T. L. Zhao, R. Arimoto, Y. Q. Wang, and Z. J. Zhou (2003), Sources of Asian dust and role of climate change versus desertification in Asian dust emission, *Geophys. Res. Lett.*, *30*(24), 2272, doi:10.1029/2003GL018206.

Zhou, Z. J., and G. C. Zhang (2003), Typical severe dust storms in northern China during 1954–2002, *Chin. Sci. Bull.*, *48*(21), 2366–2370.

X. Liu, X. Yang, and X. Zhang, SKLLQG, Institute of Earth Environment, Chinese Academy of Sciences, Xi'an, 710075 China. (liuxd@loess.llqg.ac.cn; yangxc@mail.ieecas.ac.cn; xiaoye@loess.llqg.ac.cn)

Z.-Y. Yin, Marine Science and Environmental Studies, University of San Diego, San Diego, CA 92110, USA. (zyin@sandiego.edu)